CHEMISTRY

Probing the chemistry of CdS paints in *The Scream* by in situ noninvasive spectroscopies and synchrotron radiation x-ray techniques

Letizia Monico[1,2,3]*, Laura Cartechini[1,2], Francesca Rosi[1,2], Annalisa Chieli[1,2], Chiara Grazia[1,2], Steven De Meyer[3], Gert Nuyts[3], Frederik Vanmeert[3], Koen Janssens[3,4], Marine Cotte[5,6], Wout De Nolf[5], Gerald Falkenberg[7], Irina Crina Anca Sandu[8], Eva Storevik Tveit[8], Jennifer Mass[9,10], Renato Pereira de Freitas[1,11], Aldo Romani[1,2], Costanza Miliani[1,2,12]*

The degradation of cadmium sulfide (CdS)–based oil paints is a phenomenon potentially threatening the iconic painting *The Scream* (ca. 1910) by Edvard Munch (Munch Museum, Oslo) that is still poorly understood. Here, we provide evidence for the presence of cadmium sulfate and sulfites as alteration products of the original CdS-based paint and explore the external circumstances and internal factors causing this transformation. Macroscale in situ noninvasive spectroscopy studies of the painting in combination with synchrotron-radiation x-ray microspectroscopy investigations of a microsample and artificially aged mock-ups show that moisture and mobile chlorine compounds are key factors for promoting the oxidation of CdS, while light (photodegradation) plays a less important role. Furthermore, under exposure to humidity, parallel/secondary reactions involving dissolution, migration through the paint, and recrystallization of water-soluble phases of the paint are associated with the formation of cadmium sulfates.

INTRODUCTION

The Scream motif, created by Edvard Munch between 1893 and 1916 in several versions, is one of the world's most famous representations of the existential anguish, melancholy, and loneliness of modern people. The series comprises four different versions in paint and pastel as well as a series of lithographic prints, several drawings, and sketches. The two paintings, made in 1893 and ca. 1910, are the most well-known versions and belong to the National Gallery and the Munch Museum in Oslo, respectively (*1*–*3*).

Munch described the basic experience behind the picture as follows (*4*): "I walked one evening on a road. I was tired and ill — I stood looking out across the fjord — the sun was setting — the clouds were colored red — like blood — I felt as though a scream went through nature — I thought I heard a scream. — I painted this picture — painted the clouds like real blood. The colors were screaming."

Technical examination of the two painted versions (*5*) has revealed how Munch experimented with the use of diverse binding media (tempera, oil, and pastel) in mixtures with brilliant and bold synthetic pigments from the late 18th to 19th century (such as zinc white, Prussian blue, synthetic ultramarine blue, chrome yellow, chrome green, cadmium orange, and cadmium yellow) to make "colors screaming" by combinations of brightly saturated contrasting colors and variations in the degree of glossiness of their surfaces.

The extensive use of these new colored materials poses a challenge for the long-term preservation of Munch's artworks because of their tendency to undergo (photo-)chemical transformations causing color changes and/or structural damage (*6*–*11*). The version of *The Scream* (ca. 1910) that belongs to the Munch Museum clearly exhibits signs of degradation in the sunset cloudy sky and in the neck area of the central figure, where cadmium yellow brushstrokes have altered to an off-white color, and in the lake water, where a thickly applied opaque cadmium yellow paint is affected by flaking and by paint loss (Fig. 1). This fact raised so many concerns that since 2006, after the recovery from the theft of the painting (which caused additional damage to the cardboard), it has been rarely shown to the public. Instead, it was preserved in a protected storage area, under controlled conditions of lighting, temperature (~18°C), and relative humidity (RH) (~50%).

Cadmium sulfide–based yellows ($CdS/Cd_{1-x}Zn_xS$), present in a number of artworks by masters contemporary to Edvard Munch, such as Henri Matisse (*12*–*15*), Vincent van Gogh (*16*), and James Ensor (*17*), have been documented to suffer from discoloration, flaking, and chalking of the paint films. In these cases, whitish compounds, namely, cadmium sulfate ($CdSO_4{\cdot}nH_2O$) (*12*–*17*), cadmium oxalate (CdC_2O_4) (*13*–*16*), and cadmium carbonate ($CdCO_3$) (*12*–*15*), were identified and tentatively proposed as either photodegradation products of the original cadmium yellow pigment or as residues of its synthesis process. Assessment of the condition of cadmium yellow paints is complicated by the fact that the chemical stability of these pigments may depend on their manufacturing process. Two routes, a "dry" and a "wet" method, were used for synthesizing late 19th to early 20th century cadmium yellow pigments (*18*). In the dry process, either metallic cadmium, cadmium oxide, or cadmium carbonate is calcined (ca. 300°C to 600°C) in an anoxic environment with pure sulfur in excess. The wet process involves the precipitation of one or more cadmium salts (e.g., $CdCl_2$, $CdSO_4$, and $CdCO_3$) with a soluble sulfide compound (e.g., Na_2S, H_2S, $Na_2S_2O_3$, and BaS). If a soluble zinc salt, usually with the same anion as the cadmium salt, is added

[1]CNR-SCITEC, via Elce di Sotto 8, 06123 Perugia, Italy. [2]SMAArt Centre and Department of Chemistry, Biology, and Biotechnology, University of Perugia, via Elce di Sotto 8, 06123 Perugia, Italy. [3]AXES Research Group, NANOlab Centre of Excellence, University of Antwerp, Groenenborgerlaan 171, 2020 Antwerp, Belgium. [4]Rijksmuseum, Conservation & Restoration—Scientific Research, Hobbemastraat 22, 1071 ZC Amsterdam, Netherlands. [5]ESRF, 71 Avenue des Martyrs, 38000 Grenoble, France. [6]LAMS, CNRS UMR 8220, Sorbonne Université, UPMC Univ. Paris 06, 4 place Jussieu, 75005 Paris, France. [7]DESY, Notkestraße 85, 22603 Hamburg, Germany. [8]Munch Museum, Tøyengata 53, 0578 Oslo, Norway. [9]Bard Graduate Center, 86th St., New York, NY 10024, USA. [10]Scientific Analysis of Fine Art LLC, 843 Old State Rd., Berwyn, PA 19312, USA. [11]LISComp Laboratory, Federal Institute of Rio de Janeiro, Paracambi, RJ 26600000, Brazil. [12]CNR-ISPC, via Cardinale Guglielmo Sanfelice 8, 80134 Napoli, Italy.
*Corresponding author. Email: letizia.monico@cnr.it (L.M.); costanza.miliani@cnr.it (C.M.)

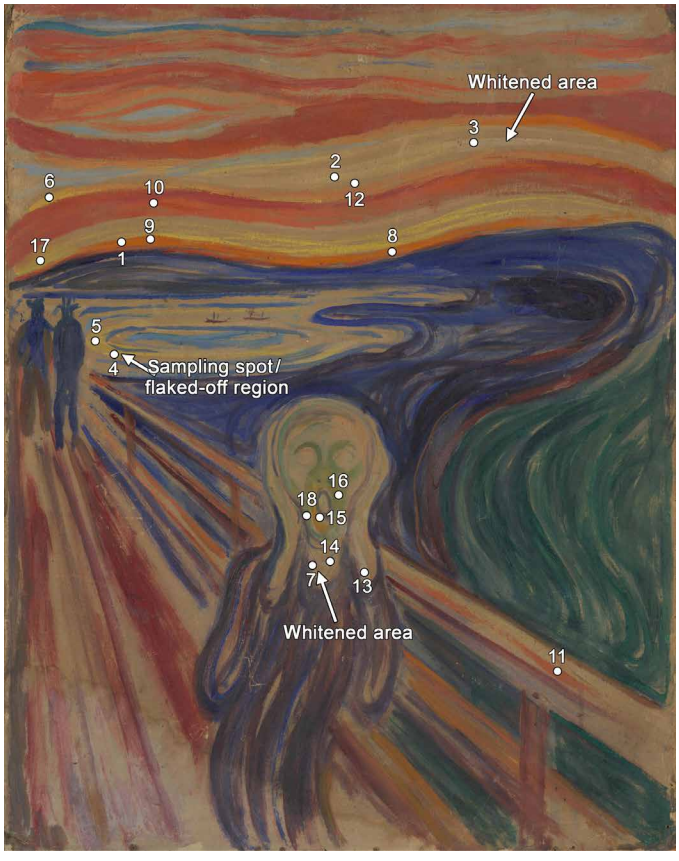

Fig. 1. Degraded cadmium yellow paints and ultraviolet–visible–near-infrared spectroscopy single-point analysis in *The Scream* (ca. 1910). Photograph of *The Scream* (ca. 1910) (Munch Museum, Oslo; catalog no. Woll.M.896) and overview of the areas where ultraviolet–visible–near-infrared (UV-vis-NIR) reflection and fluorescence spectroscopy single-point measurements were performed (see Fig. 2 and fig. S1 for the corresponding spectra). Arrows show the sampling spot and the degraded cadmium yellow paints. Photo credit: Irina Crina Anca Sandu and Eva Storevik Tveit, Munch Museum.

before precipitation, then a $Cd_{1-x}Zn_xS$ is obtained to provide different yellow hues according to the Cd/Zn ratio (*18*).

In the earlier productions based on wet processes, CdS may coexist with a number of residues of the starting reagents and/or secondary products, including various chlorine compounds [e.g., NaCl, $CdCl_2$, and Cd(OH)Cl], sulfates (e.g., Na_2SO_4 and $CdSO_4$), and $CdCO_3$ (*18*–*21*). Studies dating back to late 19th and early 20th century (*22*, *23*) have suggested that the presence of these additional components may be one of the reasons why the cadmium yellow varieties produced by the wet processes are, in general, more prone to chemical changes than those synthesized via the dry processes.

Earlier scanning electron microscopy–energy-dispersive x-ray and Fourier transform infrared (FTIR) investigations of selected microsamples of *The Scream* (ca. 1910) revealed that $CdCO_3$ is the main paint component in the paler yellow tones of the sky and the neck of the central figure, whereas the same compound was shown to be present mixed with variable amounts of S, Cl, and Na compounds in the lake region (*3*). These observations leave the following key questions to be answered: (i) Is there any correlation between the extent of degradation observed on the CdS-based paint surface and its chemical composition? (ii) What is the nature of the alteration compounds of cadmium yellow paints? (iii) Which environmental factors contribute to promote degradation of cadmium yellow paints? Finding an answer to these questions is highly relevant for setting the basis of appropriate preventive conservation strategies for *The Scream* (ca. 1910) that have the ultimate ambition to allow the painting to be returned to the public galleries of the Munch Museum.

Aimed at shedding light on these issues, we benefitted from a combination of macroscale in situ noninvasive elemental and molecular techniques (from the IR to the x-ray range) and synchrotron radiation (SR)–based x-ray microspectroscopy methods to obtain a complete overview of the different CdS-based paints used throughout *The Scream* (ca. 1910). In addition, we assessed the current condition of the paint in the lake region by analyzing a microsample by means of SR-based x-ray methods, and results were compared with outcomes arising from accelerated aging treatments (light and moisture) of a series of CdS-based oil paint mock-ups. This allowed for a deeper understanding of the role played by compositional and environmental factors on the decay of the cadmium yellow paints.

RESULTS AND DISCUSSION

Noninvasive chemical characterization and mapping of CdS-based paints in *The Scream* (ca. 1910)

A selection of results from the noninvasive analytical MOLAB campaign carried out at the Munch Museum in 2017 is presented in Fig. 2 for the scenery of the background. The macro–x-ray fluorescence (MA-XRF) elemental map of Cd (Fig. 2B) shows an extensive use of Cd-based pigments in the red, orange, and yellow hues. Selenium was detected only in a few small spots related to past restorations, thus proving that Munch, assumed to have created this painting in 1910, made use of CdS-based pigments and not of cadmium sulfur selenide ones [reported to be commercially available since 1910 (*24*)]. Ultraviolet–visible–near-IR (UV-vis-NIR) reflection and fluorescence spectroscopy, both by imaging and single-point analysis mode, with the support of FTIR reflection spectroscopy and MA-XRF mapping permitted us to differentiate three different CdS-based paints.

Paint (a)

The orange Cd-based paints (Fig. 2A, pt. 1) are characterized by UV-vis-NIR reflectance spectra with an inflection point at about 530 to 540 nm (Fig. 2D), which are not assignable to a specific CdS-based pigment because they are affected by the copresence of vermilion (α-HgS); the latter is largely present in the red/orange hues of the background landscape (fig. S1). The specific nature of the CdS pigment can be determined via analysis of its vis-NIR emission spectrum, which shows the presence of a weak fluorescence in the range 840 to 860 nm (Fig. 2D). The band is attributable to a mixture of hexagonal and cubic CdS (hereafter denoted as hex-CdS and cub-CdS, respectively; see fig. S1E) and is originated from trap states at the semiconductors' surface, called DLEs (deep-level emissions) (*19*). Strong signals of zinc oxalate ($ZnC_2O_4{\cdot}2H_2O$) were observed by FTIR (Fig. 2G). Generally, the widespread occurrence of oxalates is an evidence for oxidative stress of the binder (*25*) that, in this painting, is characterized by a lipid component variably observed in the different Cd-based paints.

Paint (b)

The paints of the sky and the neck of the central figure have altered to off-white (Fig. 2A, pts. 2 and 3, and fig. S1, pt. 7) and show UV-vis-NIR reflectance profiles very similar to those registered on the cardboard, without any clear spectral contribution due to a CdS

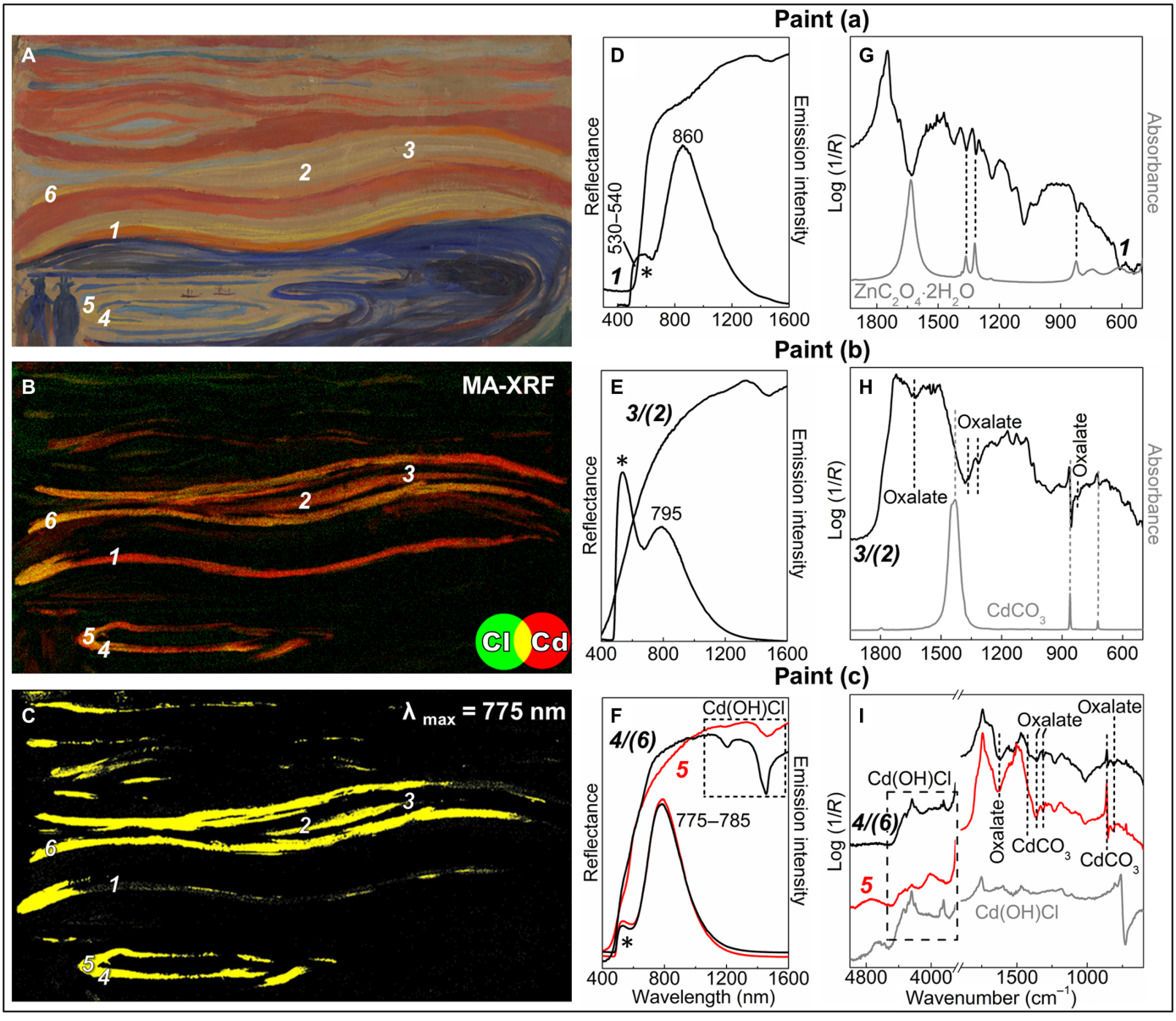

Fig. 2. Sky and lake regions: In situ noninvasive spectroscopic results. (**A**) Photograph of a detail of the sky and lake areas of *The Scream* (ca. 1910) and (**B**) corresponding composite red-green (RG) MA-XRF maps of Cd (red) and Cl (green). Photo credit: Irina Crina Anca Sandu and Eva Storevik Tveit, Munch Museum. (**C**) Spatial distribution of CdS luminescence with λ_{max} at 775 nm [Paint (c)]. (**D** to **F**) UV-vis-NIR reflectance and fluorescence spectra and (**G** to **I**) FTIR pseudo-absorbance profiles recorded from selected CdS-based areas of the sky (pts. 1 to 3 and 6) and of the lake (pts. 4 and 5) compared to those of chosen reference compounds (gray). In (E), (F), (H), and (I), numbers in brackets refer to the spectra showing similar features to those shown (see Fig. 1 and fig. S1 for additional UV-vis-NIR spectroscopy results). Asterisks in (D) to (F) indicate a signal not related to CdS but likely due to both the reflection/scattering of the excitation source and the emission of the binder and/or other fluorophores.

pigment. However, the higher sensitivity of vis-NIR fluorescence spectroscopy allowed us to detect a weak emission from residual CdS (Fig. 2E and fig. S1). The shape and position of the luminescence (λ_{max} = 790 to 795 nm) indicate the presence of hex-CdS, as shown by comparison with the spectra of powders of commercial crystalline hex-CdS and historical semicrystalline hex-CdS (fig. S1).

Paint (c)

The opaque yellow impasto paints of the sky (Fig. 2A, pt. 6) and of the lake water (Fig. 2A, pts. 4 and 5) are characterized by UV-vis-NIR reflectance profiles showing a broad sigmoidal shape (Fig. 2F), which is attributable to a low degree of crystallinity (*26*). The shape and position of the strong DLE band at λ_{max} = 775 to 785 nm suggest the main presence of hex-CdS (Fig. 2F). The paints belonging to group (c) can be spatially visualized by luminescence imaging at 775 nm (Fig. 2C). As shown by the MA-XRF maps of Cd and Cl (Fig. 2B), these areas are also characterized by a larger relative abundance of chlorine with respect to the faded off-white strokes [Paint (b)] and the orange paints [Paint (a)]. Through vis-NIR and FTIR reflection spectroscopies, chlorine is associated with the presence of cadmium

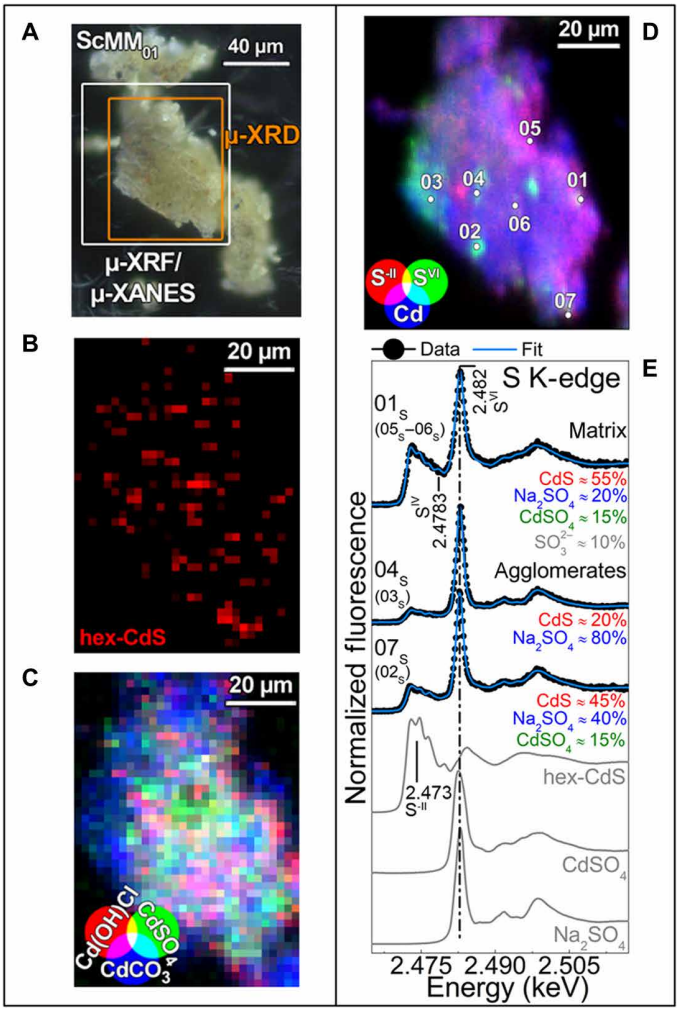

Fig. 3. Microflake ScMM$_{01}$: S speciation results. (**A**) Photomicrograph of microflake ScMM$_{01}$ taken from *The Scream* (ca. 1910) (see Fig. 1 for the sampling spot) and corresponding SR μ-XRD distribution of (**B**) hex-CdS and (**C**) Cd(OH)Cl/CdSO$_4$/CdCO$_3$ [step size (h × v), 2 × 2 μm^2; exp. time, 10 s per pixel; energy, 8.5 keV]. (**D**) Composite red-green-blue (RGB) SR μ-XRF maps of S^{-II}/S^{VI}/Cd [step size (h × v), 0.8 × 0.8 μm^2; exp. time, 100 ms per pixe]. (**E**) Selection of S K-edge spectra (black) and result of the linear combination fitting (LCF) (cyan) of different S-based compounds obtained from the spots indicated in (D). In gray, the spectral profiles of selected reference compounds are reported for comparison. Numbers in brackets refer to the spectra showing similar features to those reported (see Fig. 4 for the corresponding Cl speciation results).

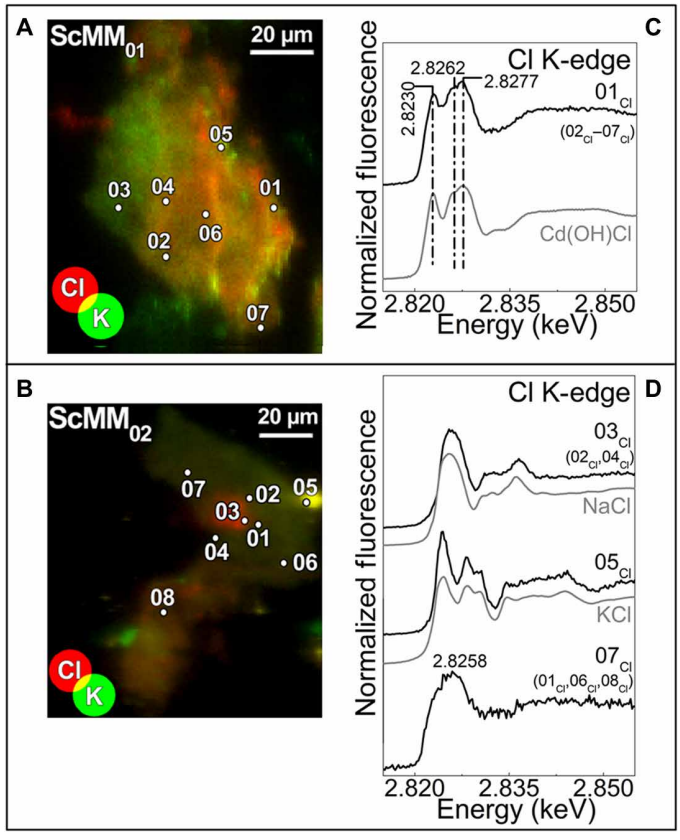

Fig. 4. Microflakes: Cl speciation results. Composite RG SR μ-XRF maps of Cl/K recorded from microflakes (**A**) ScMM$_{01}$ and (**B**) ScMM$_{02}$ [step size (h × v), 0.8 × 0.8 μm^2; exp. time, 100 ms per pixel]. Selection of the Cl K-edge spectra (black) compared to those of different Cl reference compounds (gray) obtained from (**C**) ScMM$_{01}$ and (**D**) ScMM$_{02}$. Spectral profiles were recorded from the spots indicated in (A) and (B). In (C) and (D), numbers in brackets refer to the spectra showing similar features to those reported (see Fig. 3 for the corresponding S speciation results).

hydroxychloride [Cd(OH)Cl] (Fig. 2F, band at 1455 nm; Fig. 2I, bands at 4336, 4240, and 3848 cm^{-1}). This compound was only detected (in varying amounts) in the yellow impasto of the lake and the sky (Fig. 2, A, F, and I, pts. 4 to 6).

In all the yellow CdS-based paints [Paint (b) and Paint (c)], the presence of both $CdCO_3$ and one or more types of oxalates (possibly of Zn and/or of Cd) is observed (Fig. 2, H and I). The presence of both Cd(OH)Cl and $CdCO_3$ [Paint (c)] may be related to the older practice of producing lighter shades of cadmium yellow most likely via a wet process (*18*, *21*–*23*). This hypothesis is also consistent with the low degree of crystallinity of hex-CdS, as revealed by UV-vis-NIR spectroscopy. Actually, earlier productions based on wet processes (i.e., without calcination) were found to usually yield high levels of poorly crystalline CdS (*21*).

Assessment of the degradation state of the cadmium yellow paint in the lake area

A selective microsampling of the flaking-off region of the lake area [Paint (c)] offered the opportunity to study more in depth the state of degradation of the CdS-based paint at this specific location (Fig. 1). A paint microsample was obtained by scraping the surface, resulting in six discrete micrometric flakes. All of them were directly analyzed, without any additional preparation, by μ-Raman spectroscopy and SR-based x-ray microspectroscopy methods, namely, micro–x-ray diffraction (μ-XRD), μ-XRF, and micro–x-ray absorption near-edge structure (μ-XANES) spectroscopy at S K-, Cl K-, and Cd L$_3$-edges to obtain speciation information on the S, Cd, and Cl compounds present.

The results related to two of the microflakes (ScMM$_{01}$ and ScMM$_{02}$; see Figs. 3 and 4), representative of the composition of the microsampling spot, are discussed here.

The composition of the flake ScMM$_{01}$ corroborates the noninvasive characterization, by revealing the presence of hex-CdS with a low degree of crystallinity (fig. S2) along with sparse aggregates of crystalline

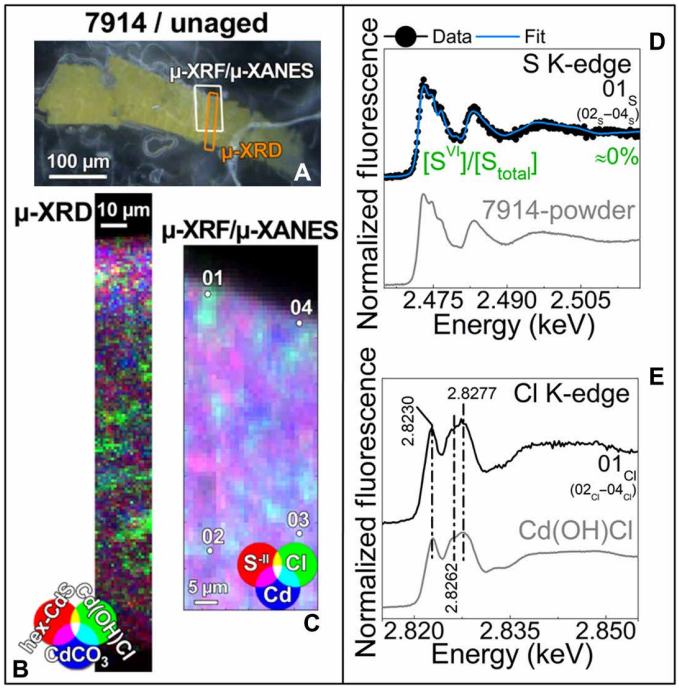

Fig. 5. Unaged early 20th century cadmium yellow oil paint mock-up (7914). (**A**) Photomicrograph of 7914 thin section before aging and corresponding RGB composite (**B**) SR μ-XRD maps of hex-CdS/Cd(OH)Cl/$CdCO_3$ [step size (h × v), 1 × 1 μm^2; exp. time, 1 s per pixel; energy, 21 keV] and (**C**) SR μ-XRF maps of S^{-II}/Cl/Cd [step size (h × v), 1×1 μm^2; exp. time, 100 ms per pixel] recorded from the area shown in (A). Selection of μ-XANES spectra at (**D**) S K-edge and (**E**) Cl K-edge obtained from the points indicated in (C) and LCF results (cyan) of different S-based reference compounds. In (D) and (E), the spectral profiles of selected reference compounds are reported in gray color for comparison, whereas numbers in brackets refer to the spectra showing similar features to those reported (see table S1 for additional results).

hex-CdS (Fig. 3B). In addition, $CdCO_3$ was found as main crystalline phase (Fig. 3C and fig. S2).

SR μ-XRF and S chemical speciation maps (Fig. 3D) reveal that Cd and S^{-II} species are homogenously distributed throughout the yellowish paint, while S^{VI} compounds are localized as agglomerates with diameter of ~3 to 12 μm. S^{-II} and S^{VI} species are unambiguously identified in the S K-edge μ-XANES spectra (Fig. 3E) by the signals at ~2.473 and ~2.482 keV, for sulfides (S^{-II}) and sulfates (S^{VI}), respectively. Moreover, the spectral feature positioned at ~2.4783 keV points toward the sporadic occurrence of sulfite (S^{IV}) compounds (*27*). Regarding flake $ScMM_{02}$, similar S speciation results were obtained (data not shown).

To determine the nature and the relative concentrations of various S species, we described each S K-edge μ-XANES spectrum as a linear combination of three to four S reference compounds [the best linear combination fitting (LCF) being obtained by including the XANES spectra of CdS, Na_2SO_3, Na_2SO_4, and/or $CdSO_4$]. Among the S-containing phases, the LCF results (Fig. 3E) reveal that the paint matrix is mainly composed of CdS, whereas sulfates with minor abundances of sulfites (Na_2SO_3) are locally present. The sulfate agglomerates consist of Na_2SO_4 along with a variable contribution of $CdSO_4$ [some of them are also revealed by SR μ-XRD (Fig. 3C)].

SR μ-XRF maps of $ScMM_{01}$ and $ScMM_{02}$ (Fig. 4, A and B) also revealed that Cl and K species are both diffused within the paint and

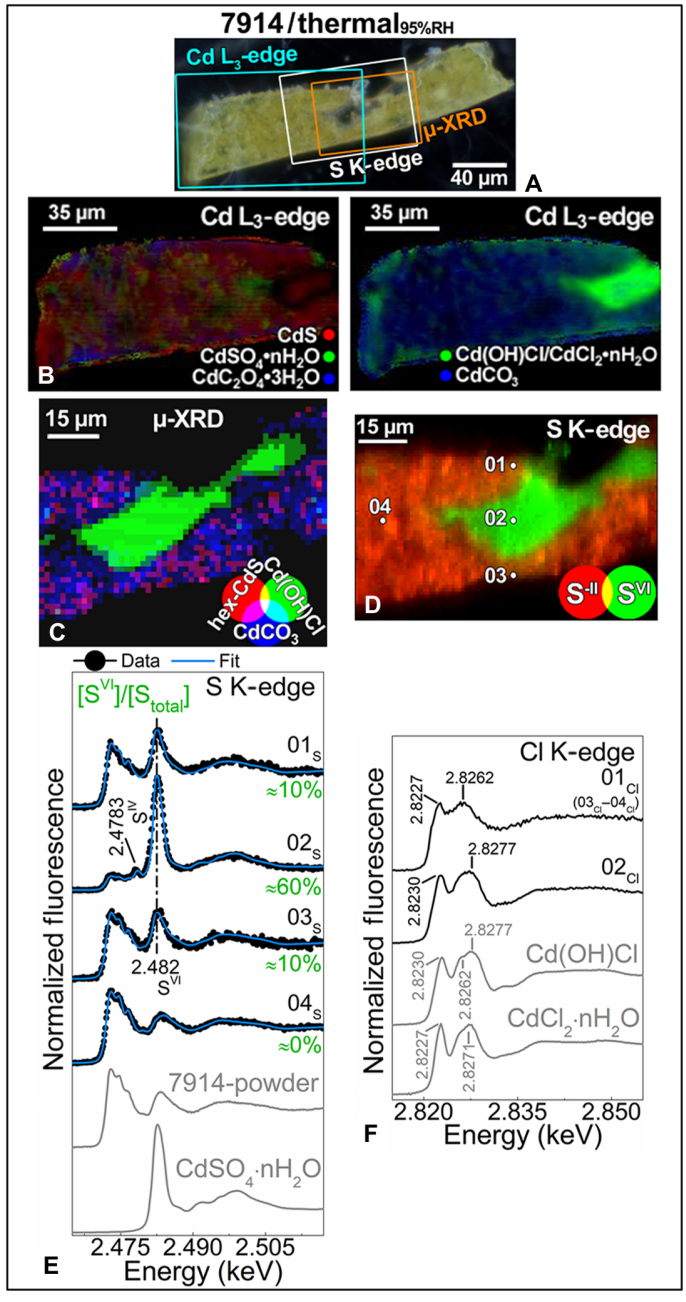

Fig. 6. Artificially aged 7914 mock-up. (**A**) Photomicrograph of 7914 thin section after thermal aging (RH ≥ 95%, T = 40°C, 90 days). (**B**) Quantitative Cd phase images obtained from the LCF of the full-field (FF)–XANES stack using the profiles of CdS (red), $CdSO_4{\cdot}nH_2O$/(Cd,Cl) chlorides (green), and $CdC_2O_4{\cdot}3H_2O$/$CdCO_3$ (blue). RGB composite (**C**) SR μ-XRD images of hex-CdS/Cd(OH)Cl/$CdCO_3$ [step size (h × v), 1.5 × 1.5 μm^2; exp. time, 1 s per pixel; energy, 21 keV] and (**D**) SR μ-XRF maps of S^{-II}/S^{VI} [step size (h × v), 1 × 1 μm^2; exp. time, 100 ms per pixel] acquired from the regions shown in (A). Selection of μ-XANES spectra at (**E**) S K-edge and (**F**) Cl K-edge obtained from the points indicated in (D) and LCF results (cyan) of different S-based reference compounds. In (E) and (F), the spectral profiles of selected reference compounds are reported in gray color for comparison, whereas numbers in brackets refer to the spectra showing similar features to those reported (see figs. S3 to S5 and table S1 for additional results).

sometimes colocalized. The series of Cl K-edge μ-XANES spectra acquired from $ScMM_{01}$ (Fig. 4C) strongly resemble the profile of Cd(OH)Cl, a compound also revealed by SR μ-XRD (Fig. 3C). In the other investigated flake (Fig. 4D), although having a similar composition, NaCl and KCl particles were also identified. In addition, in selected locations, the broad XANES feature at 2.8258 keV suggests the presence of other inorganic Cl compounds, possibly chlorides of Al, Ca, and/or Fe (SR μ-XRF maps are not shown) (*28*).

The detection of various chlorine compounds [NaCl, KCl, and Cd(OH)Cl] and $CdCO_3$ further supports the hypothesis that the semicrystalline hex-CdS pigment used here was produced by a wet process, which may explain the presence of sulfates (Na_2SO_4 and $CdSO_4$) as residues of the pigment synthesis (*18*). On the other hand, the identification of sulfites, which are reported to be intermediates of the oxidation of sulfides to sulfates (*29*), suggests that $CdSO_4$ is also an oxidation product of the original CdS pigment.

Study of CdS oxidation in oil paint mock-ups made of historical pigment formulations

To assess the effect of different environmental parameters on the oxidation process of the CdS-based oil paints on *The Scream* (ca. 1910), we studied a series of oil paint mock-ups prepared using (i) an early 20th century cadmium yellow pigment powder (henceforth referred to as "7914") from the collection of the Cultural Heritage Agency of the Netherlands (RCE) (*19*) mixed with linseed oil and (ii) an oil paint tube used by Munch himself (hereafter denoted as "LFG 2.4"), labeled *Jaune de cadmium citron* (cadmium yellow lemon) and manufactured by Lefranc (see Materials and Methods for details). The mock-ups were subjected to accelerated aging under UVA-vis light at RH = 45%, UVA-vis light at RH ≥ 95%, and thermal aging at T = 40° and RH ≥ 95% (in table S1, Figs. 5 to 7, and figs. S3 to S6 denoted as "$UVA\text{-}vis_{45\%RH}$", "$UVA\text{-}vis_{95\%RH}$", and "$thermal_{95\%RH}$", respectively). In what follows, a selection of the most meaningful results for the discussion is provided.

Early 20th century cadmium yellow pigment 7914

The historical pigment powder 7914 was specifically selected for having absorption and emission properties [fig. S1 and (*19*)] and a chemical composition similar to that of the cadmium yellow paint in the lake area. From the presence of both Cd(OH)Cl and $CdCO_3$ as additional major phases in the CdS (Fig. 5), along with a smaller amount of KCl (table S1), we infer that pigment 7914 is composed of poorly crystalline hex-CdS, possibly produced by a wet process. Neither sulfates (e.g., Na_2SO_4 and $CdSO_4$) nor sulfites (e.g., Na_2SO_3) were detected as original constituents of the pigment powder.

As a first step, we have evaluated the stability of the 7914 oil paint mock-up after exposure to UVA-vis light at RH = 45% (fig. S3). After aging, no evidence of photo-oxidation of hex-CdS to $CdSO_4$ was found, in line with our previous studies on pure CdS oil mock-ups (i.e., without any synthesis residues, such as Cl compounds) (*30*). However, the formation of cadmium carboxylates was revealed by FTIR (data not shown; see table S1 for details).

In a second step, the effects of thermal aging at RH ≥ 95% (without exposure to light) were studied. This resulted in a highly relevant phenomenon: the formation of S^{VI}-rich aggregates within the S^{-II}-based matrix, as evidenced by the S speciation distributions (Fig. 6, A and D). The LCF result of the S K-edge μ-XANES spectra (Fig. 6E) shows that the aggregate (pt. 02_S) is mainly composed of $CdSO_4/CdSO_4{\cdot}nH_2O$ and that lower amounts of the same compounds (pts. 01_S and 03_S) are sporadically present in the CdS-based matrix. In the S^{VI}-rich aggregate (pt. 02_S), an additional peak at 2.4783 keV is ascribable to SO_3^{2-} species (~15%) that are likely formed as intermediates of the oxidation process of the pigment (*29*).

These newly formed Cd species are better visualized in the full-field (FF)–XANES Cd phase images and SR μ-XRD maps (Fig. 6, B and C, and fig. S4) in which, within the hex-CdS/$CdCO_3$-based 7914 paint matrix, minor amounts of $CdC_2O_4{\cdot}3H_2O$, $CdSO_4{\cdot}nH_2O$, and $CdCl_2{\cdot}nH_2O$ are observed and localized in small aggregates (ca. 10 μm in diameter). The three latter compounds were not detected by μ-XRD, possibly because of their amorphous nature. Furthermore, the formation of Cd carboxylates was revealed by FTIR (spectra not reported; see table S1 for details).

It is notable that the results also reveal the colocalized presence of Cl species and cadmium sulfates: Cd(OH)Cl is mainly localized in the S^{VI}-rich aggregate that formed in situ during aging (Fig. 6, B to D). The μ-XRD patterns recorded from this region (fig. S5) show an extensive broadening of the Cd(OH)Cl signals compared to those that are visible in the profiles of sample 7914 before artificial aging. We assume that this is due to the nanometric crystal size of this compound (>10 nm) (*31*). In agreement with the SR μ-XRD analysis, the slight broadening and shifting toward lower energies (from 2.8277 to 2.8262 keV) of the most intense post-edge absorption feature in some Cl K-edge μ-XANES spectra (Fig. 6F) is ascribable to amorphous (Cd,Cl) compounds.

Overall, these results suggest that the original Cd(OH)Cl may have dissolved, migrated, and recrystallized as nanoparticles, possibly simultaneously with the oxidation of CdS to $CdSO_4$. Whether the presence of Cd(OH)Cl has effectively stimulated the oxidation process is not clear.

In a third experiment, the effect of combined aging, i.e., exposure to UVA-vis light and humidity (RH ≥ 95%) (data not shown; see table S1 for an overview of the results) were considered. The chemical transformations induced in this manner are very similar to those only exposed to thermal aging (Fig. 6), pointing out the dominant role of moisture on the oxidation process of the CdS-based oil paint in which (Cd,Cl) compounds are present.

In summary, the above-described findings demonstrate the joint action of (Cd,Cl) compounds and moisture in the oxidation of the CdS pigment to $CdSO_4$ in the oil binder. The results also show that the exposure to moisture promotes the migration of (Cd,Cl) species through the paint along with the oxidation of the original CdS to $CdSO_4$. Note that the formation of neither $CdSO_4$ nor cadmium carboxylates was observed on Cl-free CdS oil paint mock-ups aged under similar conditions (*30*). Therefore, this strongly suggests that the presence of Cd(OH)Cl [and possibly other (Cd,Cl) compounds] is a key factor promoting degradation of CdS. The photodegradation of CdS, on the other hand, does not appear to be influenced by the absence or presence of (Cd,Cl) compounds.

Munch's oil paint tube "cadmium yellow lemon" LFG 2.4 by Lefranc

To further explore the influence of moisture and that of the presence of (Cd,Cl) and Na compounds [the latter being observed in the available paint microflakes from *The Scream* (ca. 1910)] in a more complex paint system, we have also investigated mock-up samples prepared with the material from paint tube LFG 2.4, used by Munch. Before artificial aging, hex-CdS, cub-CdS and $CdCO_3$ are homogenously distributed throughout the paint (fig. S6). The Sulfur speciation maps (Fig. 7, A and B) in combination with S K-edge μ-XANES

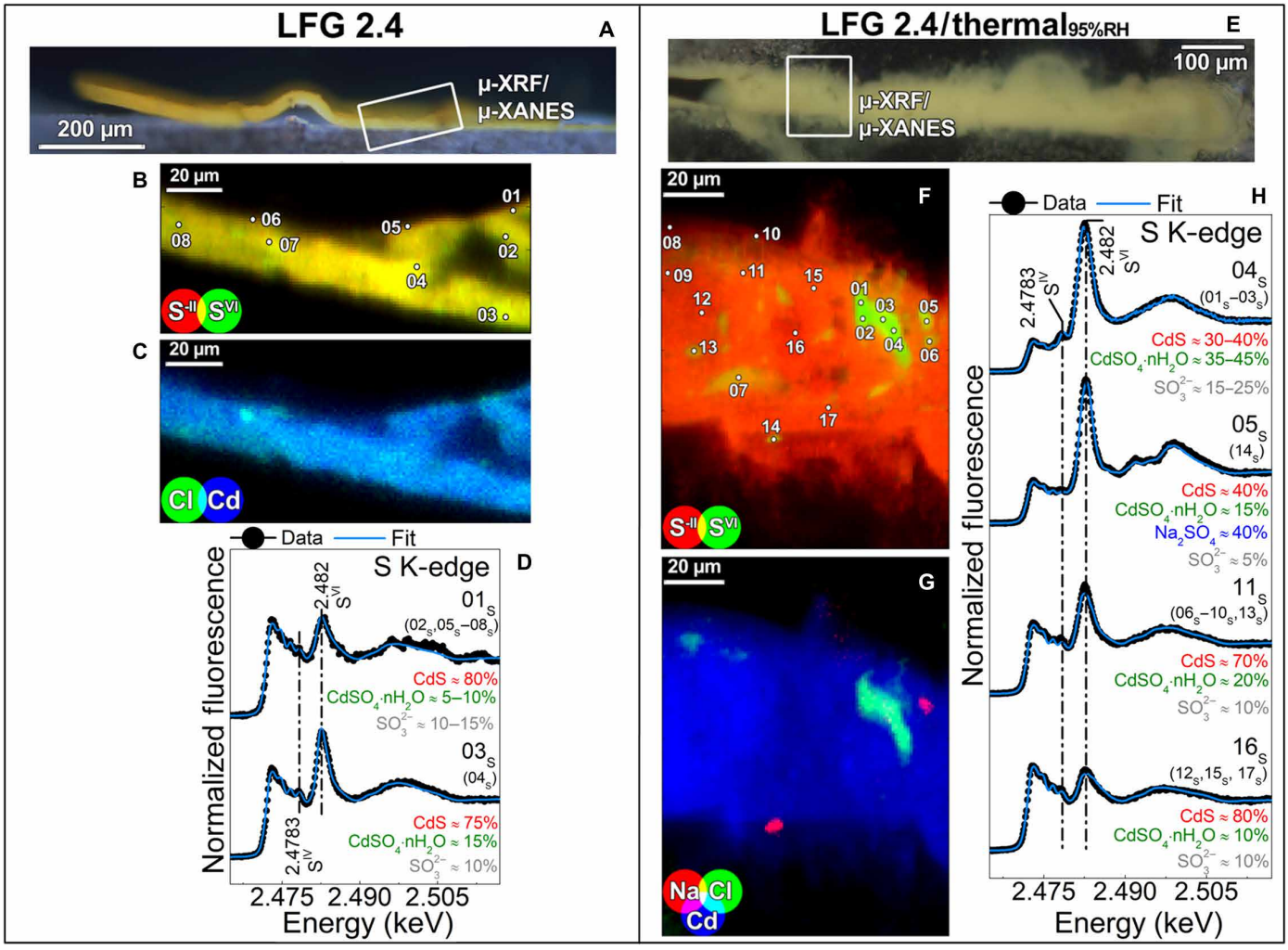

Fig. 7. Munch's cadmium yellow lemon oil paint tube (LFG 2.4). Photomicrographs of LFG 2.4 thin sections (**A**) before and (**E**) after thermal aging (RH ≥ 95%, T = 40°C, 90 days). RGB composite SR µ-XRF images of (**B**) S^{-II}/S^{VI} and (**C**) Cl/Cd [step size (h × v), 1 × 1 µm²; exp. time, 100 ms per pixel] recorded from the area shown in (A). (**D**) Selection of S K-edge µ-XANES spectra (black) obtained from the points indicated in (B) and corresponding LCF results (cyan). RGB composite SR µ-XRF images of (**F**) S^{-II}/S^{VI} and (**G**) Na/Cl/Cd [step size (*h* × *v*), 1 × 0.8 µm²; exp. time, 80 ms per pixel] acquired from the region illustrated in (E). (**H**) Selection of S K-edge µ-XANES spectra (black) obtained from the points indicated in (F) and LCF results (cyan). In (D) and (H), numbers in brackets indicate the profiles showing similar spectral features to those shown (see fig. S6 and table S1 for further results).

investigations (Fig. 7D) reveal the presence of a rather uneven distribution of S^{VI} species (likely $CdSO_4{\cdot}H_2O$; ≈5 to 15%) and S^{IV} compounds (possibly Na_2SO_3; ≈10%). These findings suggest that a partial natural aging of the paint might have already occurred during the one century lifetime of the paint tube. In addition, the presence of (Cd,Cl) compounds is revealed by µ-XRF (Fig. 7C) and Cl K-edge µ-XANES spectroscopy (data not shown), having a homogeneous distribution.

Thermal aging of the paint (RH ≥ 95%, T = 40°C, 90 days) clearly promoted the formation of Cd/S^{VI} and Na/S^{VI} aggregates [see µ-XRF maps and S speciation distributions in Fig. 7 (E to G)]. Furthermore, after aging, Cl compounds, originally homogenously distributed throughout the paint, became mainly localized in the Cd/S^{VI} aggregates (Fig. 7, F and G). In these areas, $CdSO_4{\cdot}nH_2O$ and CdS were found to be the main components along with SO_3^{2-} compounds as minor phases (Fig. 7, F and H, pts. 01_S to 04_S). In the two Na/S^{VI} aggregates (pts. 05_S and 14_S), Na_2SO_4 and CdS are the dominant phases together with smaller amounts of $CdSO_4{\cdot}nH_2O$ and possibly SO_3^{2-} compounds. This migration of the (Cd, Cl) compounds either proceeds in parallel or becomes triggered or is itself responsible for triggering the oxidation of CdS to $CdSO_4$. Other aging experiments (e.g., with observation at the nanoscale of Cl-containing CdS) are required (and planned) to obtain definite insights in this matter.

The identification of highly water-soluble materials such as Na_2SO_4 and (Cd,Cl) compounds, both in the LFG 2.4 paint and in the microflakes from *The Scream* (Figs. 3 and 4), also leads to the question of whether and to what extent their solubility influences the degradation state of the cadmium yellow paint under high humidity conditions. This was further investigated by thermal aging (RH ≥ 95%, T = 40°C) of two oil paint mock-ups prepared by mixing pure hex-CdS with Na_2SO_4 and $CdCl_2$. The results (see section S4 for details) confirmed that after exposure to moisture, soluble Na_2SO_4 and $CdCl_2$ dissolve, migrate through the paint, and, upon recrystallization, give rise to $CdSO_4$- and NaCl-based compounds. It follows that cadmium sulfate may be present

not only as an oxidation product of CdS or as a direct leftover reagent but also as a secondary product arising from the dissolution and recrystallization of soluble sulfate-containing leftover reagents.

CONCLUSIONS

A two-length scale approach has been presented here to investigate the chemistry of CdS-based pigments of *The Scream* (ca. 1910) by combining noninvasive elemental and molecular spectroscopies at the macroscale with SR–based x-ray methods at the microscopic level. The results from the extensive in situ noninvasive investigation provided us with a representative overview of the chemical composition and distribution of the different CdS-based paints used by Munch in his masterpiece. Notably, two different types of the cadmium yellow pigment were identified: poorly crystalline hex-CdS and cub-CdS.

Evidence of degradation either in the form of flaking detachment (opaque yellow impasto paints of the lake water) or discoloration to an off-white color (in the sunset sky area and the neck region of the central figure) was primarily observed for CdS yellow oil paints made of hex-CdS pigments that exhibit a low degree of crystallinity and contain significant amounts of $CdCO_3$ along with a variable content of chlorine compounds. The compositional profile has revealed the use of a CdS yellow pigment produced by the wet process without calcination. On the other hand, orange paints, composed of a mixture of hex-CdS/cub-CdS and variable amount of HgS, without $CdCO_3$- and Cl-based compounds, do not show evident signs of degradation.

Insight into the nature of the alteration compounds present in the flaking impasto paint was provided by microspectroscopy investigations of a microsample obtained from the lake area. The most important result was the first ever reported evidence of the presence of oxidized sulfur compounds in the CdS-based paints of *The Scream* (ca. 1910). Notably, variable amounts of $CdSO_4$ and sulfites species were found to be widespread throughout the paint matrix, whereas Na_2SO_4 was present in the form of aggregates. Different chloride-based compounds, including Cd(OH)Cl, NaCl, and KCl, were identified as well.

The combination of these results with the findings obtained from artificially aged paint mock-ups (with a composition similar to that of the lake region of the painting) leads us to conclude that the sulfates and sulfites can be interpreted as alteration products of the paint. As the most important outcome of this study, we observed that in high moisture conditions (RH $\geq$ 95%) and in the presence of different types of cadmium chloride compounds, the oxidation of the original CdS to $CdSO_4$ also takes place in the absence of light. Whether the migration of (Cd,Cl) compounds is a cause or an effect of the CdS oxidation or simply takes place in parallel is not yet resolved. This observation has opened the way for a targeted research on the oxidation mechanism of CdS-based pigments in oil binder under high moisture conditions and in the presence of various chloride compounds (e.g., KCl, NaCl, $CdCl_2{\cdot}nH_2O$, and $CdCl_2$). Studies are still ongoing, and their results will be published in follow-up papers.

Upon exposure to humidity, next to the oxidation of the original CdS pigment, secondary reactions involving dissolution, migration through the paint, and recrystallization of water-soluble phases such as Na_2SO_4 and Cd(OH)Cl/$CdCl_2$ may have further contributed to the formation of cadmium sulfates and of various Cl compounds. The nature and distribution of the water-soluble and "mobile" phases determined in the sampled material from *The Scream* (ca. 1910) contribute to explain the instability of the paint in the lake area and the related flaking issue.

Overall, we consider that our findings provided important clues about the degradation mechanism of CdS-based paints, having meaningful implications for the preventive conservation of *The Scream* (ca. 1910). In particular, the degradation of the cadmium yellow paints might be mitigated by minimizing the exposure of the painting to excessively high moisture levels (i.e., RH < 45%) while keeping the lighting at normal values foreseen for lightfast painting materials (*32*).

MATERIALS AND METHODS

The Scream (ca. 1910) (Munch Museum, Oslo, Norway) and corresponding microsample

The version of *The Scream* (ca. 1910) (tempera and oil on unprimed cardboard, 83.5 cm by 66 cm; catalog no. Woll.M.896) belonging to the Munch Museum is neither signed nor dated. Earlier research has established that the painting probably stems from around 1910 (*1*–*3*). The painting, stolen in 2004, has been extensively studied since its return at the Munch Museum in 2006 (*3*, *5*).

The paint microsample that was studied was taken from a spot of the flaked-off yellow paint surface of the lake region in the painting (Fig. 1). It was obtained by scraping the surface, resulting in six discrete micrometric flakes; all of them were directly investigated without any additional preparation. The results obtained from two of them ($ScMM_{01}$ and $ScMM_{02}$; see Figs. 3 and 4), representative of the composition of the microsampling location, are discussed above.

Preparation of CdS-based oil paint mock-ups

Early 20th century cadmium yellow pigment

The pigment powder (sample "7914") is dated back to the early 20th century and was provided by the RCE. Paint mock-ups were obtained by mixing the pigment powder, composed of $CdCO_3$, Cd(OH)Cl, KCl, and poorly crystalline hex-CdS [see table S1 and (*19*) for further information], with linseed oil (Zecchi) in a 4:1 mass ratio and applied on polycarbonate slices.

Munch's oil paint tube

The analyzed sample (LFG 2.4; table S1 and Fig. 7), produced by Lefranc (Paris) and labeled as *Jaune de cadmium citron* (cadmium yellow lemon), is from the collection of oil paint tubes (more than 900 in total) that Edvard Munch (1863 to 1944) used in the last period of his life, in the atelier in Ekely (1916 to 1944). It is likely that some paint materials were bought before these dates (*3*). The tubes are part of a corpus of atelier materials that the painter donated to the city of Oslo after his death, now hosted at the Munch Museum. The paint sample (less than 1 g) was obtained by softly squeezing the paint tube (still with cap; fig. S6A) in small vials; afterward, this paint was applied on a polycarbonate support.

Commercial hex-CdS pigment

Paint mock-ups were prepared by mixing powders of crystalline hex-CdS (Sigma-Aldrich) with an equal amount of both Na_2SO_4 and $CdCl_2$ (sample "hex-$CdS_{Na_2SO_4\text{-}CdCl_2}$") in a 4:1 mass ratio (table S1 and figs. S7 and S8). A blend of the powder mixtures with linseed oil (4:1 mass ratio) was applied on areas of about 1.5 cm by 1.5 cm on a polycarbonate support.

Accelerated aging experiments of CdS-based oil paint mock-ups

UVA-vis photochemical aging experiments of the 7914 oil paint mock-ups were carried out by allocating the touch-dried paints (i.e., after about 1 month since their preparation) inside an in-house–made

aging chamber equipped with a UV-filtered 300-W Cermax xenon lamp [$\lambda \geq 300$ nm; see (*33*) for the corresponding emission spectral profile] either at RH = 45% (indoor humidity level, measured daily using a thermohygrometer) or at RH ≥ 95% (obtained using distilled water). These aging conditions are referred to as UVA-vis$_{45\%RH}$ and UVA-vis$_{95\%RH}$, respectively. The measured irradiance and temperature at the sample position were 1.8×10^3 to 2.7×10^3 W/m^2 and 25° to 30°C, respectively. Paints were irradiated for 430 to 640 hours to achieve radiant exposure values of ca. 1.2×10^6 W/m^2·hour. Thermal aging treatments (denoted as "thermal$_{95\%RH}$") of all CdS-based oil paint mock-ups were performed by placing the touch-dried paints in a vessel maintained in the dark at RH ≥95% (obtained using distilled water) and at 40°C for an overall period of 90 to 100 days (2160 to 2400 hours).

MA-XRF mapping

MA-XRF scanning was carried out using the CRONO instrument by XGLab (Bruker Nano Analytics) (*34*). The system has a measurement head equipped with a large area silicon drift detector and a Rh anode tube operating at 50 kV and 200 μA. The measurement head is mounted on a motorized *XYZ* stage (scanning area, 450 mm by 600 mm and focusing axis, 75 mm). The painting was scanned using a 1-mm pinhole collimator with a linear speed of 20 mm/s and acquisition time of 40 ms per spectrum. XRF elemental maps were produced by the PyMca (*35*) and Datamuncher (*36*) software packages.

Fluorescence hyperspectral imaging

Two Honle LEDLINE 500 light-emitting diode systems with emission at 405 nm were used as excitation sources for the luminescence measurements. Investigations were performed by means of a Surface Optics Corporation SOC710 hyperspectral camera. The system uses a whiskbroom line scanner, producing a 696 × 520 pixels hypercube in the spectral range of 400 to 1000 nm, with 128 bands and 4.5 nm spectral resolution, radiometrically calibrated in the whole spectral range. The lateral resolution was continuously modulated by an adjustable focal length of the mounted objective. The fluorescence hypercube of the whole painting has been reconstructed by assembling 15 single frames collected at a resolution of about 70 dots per inch, using the pixel-based mosaicking routine present in the ENVI Classic software. From the whole hyperspectral fluorescence image, any single spectral band (i.e., band at 775 nm of Fig. 2C) was mapped by adjusting the brightness to obtain the dark (or zero) contribution from an area that clearly does not contain the species emitting at the selected spectral band.

UV-vis-NIR measurements

UV-vis-NIR reflection and fluorescence investigations at selected locations of the painting were performed by a self-assembled portable instrument. A deuterium-halogen lamp (AvaLight-DHc, Avantes), a highly sensitive charge-coupled device (CCD) spectrometer (AvaSpec-2048 USB2, Avantes; range, 200 to 1100 nm and spectral resolution, 8 nm), and a thermoelectrically cooled InGaAs detector (AvaSpec-NIR256-1.7TEC; range, 950 to 1600 nm and spectral resolution, 24 nm) were used for carrying out reflection measurements. An ultracompact diode laser (Toptica Photonics AG, DE; 445 nm, 1-mW nominal power), integrated into the same apparatus and coupled with two high-sensitivity calibrated CCD spectrometers (i.e., AvaSpec-NIR256-1.7TEC and AvaSpec-ULS2048 XL-RS-USB2; range, 300 to 1150 nm and spectral resolution, 9.2 nm), was used for performing fluorescence measurements. The instrument has a dedicated fiber-optic system, designed to direct all the excitation sources to the same point of the analyzed surface and, at the same time, collect both the reflected and emitted light, bringing them to the different detectors. The probe area is less than 2 mm^2. Measurements were carried out with an integration time of 600 ms and 30 averages for each acquisition.

FTIR measurements

A portable ALPHA spectrometer (Bruker) was used for performing reflection investigations at selected spots of the painting and attenuated total reflection (ATR) measurements at the surface of all CdS-based oil paint mock-ups before and after aging. Pseudo-absorbance spectra [log(1/*R*); *R* is reflectance] were obtained using an external reflection module from areas of about 7 mm^2. Data were acquired in the range of 7400 to 345 cm^{-1}, at a resolution of 4 cm^{-1} and for 3 min.

ATR spectra were collected by means of a Platinum QuickSnap ATR sampling module (A220/D-01) equipped with a diamond crystal plate. Data were recorded in the range of 4000 to 345 cm^{-1}, with 4 cm^{-1} spectral resolution and 168 scans.

μ-Raman investigations

Microflakes obtained from *The Scream* (ca. 1910) and thin sections (~5 μm in thickness) prepared from hex-CdS$_{Na_2SO_4\text{-}CdCl_2}$ paint mock-ups were investigated by means of a JASCO NRS-3100 double-grating spectrophotometer. The instrument is connected to an optical microscope (×100 objective) and is equipped with a CCD detector cooled down to −47°C.

The analyses were performed using a 514.5 nm argon-ion laser and a grating with 1200 lines/mm. Profiles were collected in the range of 2130 to 120 cm^{-1}, with ca. 2 cm^{-1} spectral resolution, 2 to 3 s exposure time, 40 to 60 scans, and 0.4 to 1 mW power.

Mapping experiments of paint mock-ups before and after thermal aging were performed by recording the spectra point by point by means of a 785.0 nm diode laser and with step size down to 2×1 μm^2 ($h \times v$). Each profile was acquired in the range of 1855 to 120 cm^{-1}, with a spectral resolution between 2 and 4 cm^{-1} and by using a grating with 600 lines/mm . The exposure time varied between 3 and 4 s per point, with three scans per point and 7 to 8 mW power.

SR-based μ-XRF and XANES measurements

S, Cl, and Cd speciation investigations of the microflakes obtained from *The Scream* (ca. 1910) and thin sections (5 to 10 μm in thickness) of CdS-based oil paint mock-ups were performed at the scanning x-ray microscope (SXM) and the FF-XANES end stations hosted at the X-ray Microscope Beamline ID21 of the European Synchrotron Radiation Facility (ESRF, Grenoble, France) (*37*). Investigations were carried out by means of a fixed exit double-crystal Si(111) monochromator at both the SXM and FF-XANES end stations. The energy calibration was performed using $CaSO_4{\cdot}2H_2O$, NaCl, and a Cd foil as standards and by setting the position of the peak maximum of their first-order derivative spectrum at 2.4829, 2.8261, and 3.5418 keV, respectively.

At the SXM-end station, the incident beam was focused with Kirkpatrick-Baez mirrors down to a diameter of 0.6×0.3 μm^2 ($h \times v$). XRF signals were collected at 69° with respect to the incident beam direction by means of a single energy-dispersive silicon drift detector (XFlash 5100, Bruker).

Single-point μ-XANES spectra were acquired in XRF mode by scanning the primary energy at the absorption edge of the following

elements: S K-edge (2.46 to 2.53 keV; energy step, 0.18 eV), Cl K-edge (2.79 to 2.89 keV; energy step, 0.25 eV), and Cd L_3-edge (3.5 to 3.7 keV; energy step, 0.4 eV).The normalization and the LCF of the spectra against a library of XANES spectra of S, Cl, and Cd reference compounds were performed by means of the ATHENA software (*38*). The LCF procedure permitted to quantitatively determine the average relative amount of sulfate (S^{VI}), sulfite (S^{IV}), and sulfide (S^{-II}) compounds (expressed as %[S^{VI}]/[S_{total}], %[S^{IV}]/[S_{total}], and %[S^{-II}]/[S_{total}]) and of different Cd and Cl compounds. During the S K-edge μ-XANES analysis, care was taken to ensure that the sulfite-related signals were not artifacts of the measurement process (e.g., due to beam-induced reduction of sulfates).

μ-XRF mapping experiments were performed by using a monochromatic primary beam of fixed energy around the S K- and Cd L_3-edges. Maps of the same region of interest were recorded using either 80 or 100 ms per pixel at three different energies: (i) 2.473 and 2.482 keV to favor the excitation of the S^{-II} and S^{VI} species, respectively, and (ii) 3.7 keV to obtain the XRF intensity of all S, Cl, and Cd species. The software PyMca (*35*) was used to fit the XRF spectra and to separate the contribution of different elements. The experimental procedure used for recording and producing the S^{-II} and S^{VI} chemical state maps is described in a previous study (*17*).

Cd L_3-edge FF-XANES imaging of a thin section (~2 μm in thickness) obtained from the thermally aged paint 7914 was carried out by means of an unfocused beam (size of ~1.5 mm by 1.5 mm). A Lu_2SiO_5:Tb scintillator (located less than 2 mm downstream the sample) was used to convert x-ray transmission images into visible images. A ×10 optical objective was used to magnify the image onto a complementary metal-oxide semiconductor camera (PCO edge, Germany), giving a pixel size of ~0.65 μm by 0.65 μm and a spatial resolution of ~1.5 μm. The maximum field of view is around 1.5 mm by 1.5 mm. A stack of 214 x-ray radiographs was recorded while tuning the x-ray energy across the Cd L_3-edge with the following variable step sizes: (i) 5 eV in the range of 3.4880 to 3.5239 keV and 3.6380 to 3.7180 keV, (ii) 0.5 eV in the region of 3.2530 to 3.5980 keV, and (iii) 1 eV in the range of 3.5980 to 3.6380 keV. The dark- and flat-field correction and the image alignment were performed by using the Spectrocrunch library (*37*). The TXM-Wizard software package (*39*) was used to produce the chemical state maps of different Cd compounds. After determination of the edge-jump, noise filtering, and normalization, Cd phase maps were obtained by describing the XANES spectra at each pixel as LCF of a set of XANES spectra of different Cd reference compounds.

SR-based μ-XRD mapping

Microflakes obtained from *The Scream* (ca. 1910) were analyzed at the μ-XRD/μ-XRF end station of beamline ID21 at ESRF (*37*), whereas thin sections of the CdS-based oil paint mock-ups were investigated at the microprobe hutch of the Hard X-ray Micro/Nanoprobe beamline P06 of the PETRA III storage ring (DESY, Hamburg) (*40*). Incident energies of 8.53 and 21 keV were used at ESRF-ID21 and DESY-P06, respectively, and were selected by means of a Si(111) crystal monochromator. A Kirkpatrick-Baez mirror system was used to focus the beam down to 2 × 1 μm^2 ($h \times v$) and down to around 0.7 × 0.7 μm^2 ($h \times v$) during the investigations at ESRF-ID21 and DESY-P06, respectively. XRD signals were recorded in transmission geometry using two different detection systems: a taper optics CCD 'FReLoN' camera (2048 × 2048 pixels, pixel size of 52 μm) was used during the analysis at ESRF-ID21, while a PILATUS 300K area detector was used for measurements at DESY-P06. μ-XRD patterns were acquired with either 10 or 1 s per pixel at ESRF-ID21 and DESY-P06, respectively. Calibration of the diffraction setups was performed using either a corundum (Al_2O_3) or a LaB_6 reference sample at ESRF-ID21 and DESY-P06, respectively. Crystalline phase distribution maps were obtained by full pattern refinement using the XRDUA software package (*41*).

SUPPLEMENTARY MATERIALS

Supplementary material for this article is available at http://advances.sciencemag.org/cgi/content/full/6/20/eaay3514/DC1

REFERENCES AND NOTES

1. G. Woll, *Edvard Munch: Complete Paintings. Catalogue Raisonne* (Thames and Hudson, 2009), vol. 4.
2. G. Woll, *Edvard Munch: The Complete Graphic Works* (Orfeus Publishing, Oslo and Philip Wilson Publishers, revised ed., 2012).
3. T. Froysaker, N. Streeton, H. Kutzke, F. Hanssen-Bauer, B. Topalova-Casadiego, *Public Paintings by Edvard Munch and His Contemporaries: Change and Conservation Challenges* (Archetype Publications Ltd, 2015), pp. 3–35, 52–71, 204–216, 294–324.
4. A. Eggum, *The Masterworks of Edvard Munch* (Museum of Modern Art, 1979), p. 30.
5. B. Singer, T. E. Aslaksby, B. Topalova-Casadiego, E. S. Tveit, Investigation of materials used by Edvard Munch. *Stud. Conserv.* **55**, 274–292 (2010).
6. C. Miliani, L. Monico, M. J. Melo, S. Fantacci, E. M. Angelin, A. Romani, K. Janssens, Photochemistry of artists' dyes and pigments: Towards better understanding and prevention of colour change in works of art. *Angew. Chem. Int. Ed.* **57**, 7324–7334 (2018).
7. L. Monico, L. Sorace, M. Cotte, W. De Nolf, K. Janssens, A. Romani, C. Miliani, Disclosing the binding medium effects and the pigment solubility in the (photo)reduction process of chrome yellows ($PbCrO_4$/$PbCr_{1-x}S_xO_4$). *ACS Omega* **4**, 6607–6619 (2019).
8. F. Gabrieli, F. Rosi, A. Vichi, L. Cartechini, L. Pensabene Buemi, S. G. Kazarian, C. Miliani, Revealing the nature and distribution of metal carboxylates in Jackson Pollock's *Alchemy* (1947) by micro-attenuated total reflection FT-IR spectroscopic imaging. *Anal. Chem.* **89**, 1283–1289 (2017).
9. L. Baij, J. J. Hermans, K. Keune, P. Iedema, Time-dependent ATR-FTIR spectroscopic studies on fatty acid diffusion and the formation of metal soaps in oil paint model systems. *Angew. Chem. Int. Ed.* **57**, 7351–7354 (2018).
10. E. Cato, C. Borca, T. Huthwelker, E. S. Ferreira, Aluminium X-ray absorption near-edge spectroscopy analysis of discoloured ultramarine blue in 20th century oil paintings. *Microchem. J.* **126**, 18–24 (2016).
11. E. R. de la Rie, A. Michelin, M. Ngako, E. Del Federico, C. Del Grosso, Photo-catalytic degradation of binding media of ultramarine blue containing paint layers: A new perspective on the phenomenon of "ultramarine disease" in paintings. *Polym. Degrad. Stab.* **144**, 43–52 (2017).
12. J. L. Mass, R. Opila, B. Buckley, M. Cotte, J. Church, A. Mehta, The photodegradation of cadmium yellow paints in Henri Matisse's *Le Bonheur de vivre* (1905–1906). *Appl. Phys. A* **111**, 59–68 (2013).
13. J. Mass, J. Sedlmair, C. S. Patterson, D. Carson, B. Buckley, C. Hirschmugl, SR-FTIR imaging of the altered cadmium sulfide yellow paints in Henri Matisse's *Le Bonheur de vivre* (1905–6)–examination of visually distinct degradation regions. *Analyst* **138**, 6032–6043 (2013).
14. Z. E. Voras, K. deGhetaldi, M. B. Wiggins, B. Buckley, B. Baade, J. L. Mass, T. P. Beebe Jr., ToF–SIMS imaging of molecular-level alteration mechanisms in *Le Bonheur de vivre* by Henri Matisse. *Appl. Phys. A* **121**, 1015–1030 (2015).
15. E. Pouyet, M. Cotte, B. Fayard, M. Salomé, F. Meirer, A. Mehta, E. S. Uffelman, A. Hull, F. Vanmeert, J. Kieffer, M. Burghammer, K. Janssens, F. Sette, J. Mass, 2D X-ray and FTIR micro-analysis of the degradation of cadmium yellow pigment in paintings of Henri Matisse. *Appl. Phys. A* **121**, 967–980 (2015).
16. G. Van der Snickt, K. Janssens, J. Dik, W. De Nolf, F. Vanmeert, J. Jaroszewicz, M. Cotte, G. Falkenberg, L. Van der Loeff, Combined use of synchrotron radiation based micro-X-ray fluorescence, micro-X-ray diffraction, micro-X-ray absorption near-edge, and micro-fourier transform infrared spectroscopies for revealing an alternative degradation pathway of the pigment cadmium yellow in a painting by Van Gogh. *Anal. Chem.* **84**, 10221–10228 (2012).
17. G. Van der Snickt, J. Dik, M. Cotte, K. Janssens, J. Jaroszewicz, W. De Nolf, J. Groenewegen, L. Van der Loeff, Characterization of a degraded cadmium yellow (CdS) pigment in an oil painting by means of synchrotron radiation based X-ray techniques. *Anal. Chem.* **81**, 2600–2610 (2009).
18. I. Fiedler, M. Bayard, Cadmium yellows, oranges and reds, in *Artist's Pigments: A Handbook of their History and Characteristics*, R. L. Feller Ed. (National Gallery of Art, 1986), vol. 1, pp. 65–108.

19. F. Rosi, C. Grazia, F. Gabrieli, A. Romani, M. Paolantoni, R. Vivani, B. G. Brunetti, P. Colomban, C. Miliani, UV–vis-NIR and micro Raman spectroscopies for the non destructive identification of $Cd_{1-x}Zn_xS$ solid solutions in cadmium yellow pigments. *Microchem. J.* **124**, 856–867 (2016).
20. M. Ghirardello, S. Mosca, J. Marti-Rujas, L. Nardo, A. Burnstock, A. Nevin, M. Bondani, L. Toniolo, G. Valentini, D. Comelli, Time-resolved photoluminescence microscopy combined with X-ray analyses and Raman spectroscopy sheds light on the imperfect synthesis of historical cadmium pigments. *Anal. Chem.* **90**, 10771–10779 (2018).
21. B. Leone, A. Burnstock, C. Jones, P. Hallebeek, J. Boon, K. Keune, *Preprints of the ICOM-CC 14th Triennial Meeting* (James & James, 2005), pp. 803–813.
22. A. H. Church, *The Chemistry of Paints and Painting* (Seeley, Service & Co. Limited, 1915), pp. 162–167.
23. A. P. Laurie, *Facts About Processes, Pigments, and Vehicles: A Manual for Art Students* (London Macmillan & Co., 1895), pp. 51–52.
24. R. J. Gettens, G. L. Stout, *Painting Materials: A Short Encyclopedia* (Dover, 1966), p. 101.
25. F. Rosi, L. Cartechini, L. Monico, F. Gabrieli, M. Vagnini, D. Buti, B. Doherty, C. Anselmi, B. G. Brunetti, C. Miliani, *Metal Soaps in Art: Conservation and Research*, F. Casadio, K. Keune, P. Noble, A. van Loon, E. Hendriks, S. Centeno, G. Osmond Eds. (Springer International Publishing, 2019), pp. 173–193.
26. H. Deng, J. M. Hossenlopp, Combined X-ray diffraction and diffuse reflectance analysis of nanocrystalline mixed Sn(II) and Sn(IV) oxide powders. *J. Phys. Chem. B.* **109**, 66–73 (2005).
27. G. Almkvist, K. Boye, I. Persson, K-edge XANES analysis of sulfur compounds: An investigation of the relative intensities using internal calibration. *J. Synchrotron Radiat.* **17**, 683–688 (2010).
28. F. Zhu, M. Takaoka, K. Shiota, K. Oshita, Y. Kitajima, Chloride chemical form in various types of fly ash. *Environ. Sci. Technol.* **42**, 3932–3937 (2008).
29. D. Meissner, R. Memming, B. Kastening, Photoelectrochemistry of cadmium sulfide. 1. Reanalysis of photocorrosion and flat-band potential. *J. Phys. Chem.* **92**, 3476–3483 (1988).
30. L. Monico, A. Chieli, S. De Meyer, M. Cotte, W. De Nolf, G. Falkenberg, K. Janssens, A. Romani, C. Miliani, Role of the relative humidity and the Cd/Zn stoichiometry in the photooxidation process of cadmium yellows ($CdS/Cd_{1-x}Zn_xS$) in oil paintings. *Chemistry* **24**, 11584–11593 (2018).
31. B. D. Cullity, *Elements of X-ray Diffraction* (Addison-Wesley Publishing Company Inc., 1967).
32. Commission Internationale de L'Eclairage, *Control of Damage to Museum Objects by Optical Radiation* (The Commission, Vienna, Austria, 2004).
33. L. Monico, K. Janssens, M. Cotte, A. Romani, L. Sorace, C. Grazia, B. G. Brunetti, C. Miliani, Synchrotron-based X-ray spectromicroscopy and electron paramagnetic resonance spectroscopy to investigate the redox properties of lead chromate pigments under the effect of visible light. *J. Anal. At. Spectrom* **30**, 1500–1510 (2015).
34. R. Alberti, T. Frizzi, L. Bombelli, M. Gironda, N. Aresi, F. Rosi, C. Miliani, G. Tranquilli, F. Talarico, L. Cartechini, CRONO: A fast and reconfigurable macro x-ray fluorescence scanner for in-situ investigations of heritage objects. *X-ray Spectrom.* **46**, 297–302 (2017).
35. M. Cotte, T. Fabris, G. Agostini, D. Motta Meira, L. De Viguerie, V. A. Solé, Watching kinetic studies as chemical maps using open-source software. *Anal. Chem.* **88**, 6154–6160 (2016).
36. M. Alfeld, K. Janssens, Strategies for processing mega-pixel x-ray fluorescence hyperspectral data: A case study on a version of Caravaggio's painting Supper at Emmaus. *J. Anal. At. Spectrom* **30**, 777–789 (2015).
37. M. Cotte, E. Pouyet, M. Salome, C. Rivard, W. De Nolf, H. Castillo-Michel, T. Fabris, L. Monico, K. Janssens, T. Wang, P. Sciau, L. Verger, L. Cormier, O. Dargaud, E. Brun, D. Bugnazet, B. Fayard, B. Hesse, A. P. del Real, G. Veronesi, J. Langlois, N. Balcar, Y. Vandenberghe, V. A. Sole, J. Kieffer, R. Barrett, C. Cohen, C. Cornu, R. Baker, E. Gagliardini, E. Papillon, J. Susini, The ID21 X-ray and infrared microscopy beamline at the ESRF: Status and recent applications to artistic materials. *J. Anal. At. Spectrom.* **32**, 477–493 (2017).
38. B. Ravel, M. J. Newville, ATHENA, ARTEMIS, HEPHAESTUS: Data analysis for X-ray absorption spectroscopy using IFEFFIT. *J. Synchrotron Radiat.* **12**, 537–541 (2005).
39. Y. Liu, F. Meirer, P. A. Williams, J. Wang, J. C. Andrews, P. Pianetta, TXM-Wizard: A program for advanced data collection and evaluation in full-field transmission X-ray microscopy. *J. Synchrotron Radiat.* **19**, 281–287 (2012).
40. U. Boesenberg, C. G. Ryan, R. Kirkham, D. P. Siddons, M. Alfeld, J. Garrevoet, T. Núñez, T. Claussen, T. Kracht, G. Falkenberg, Fast X-ray microfluorescence imaging with submicrometer-resolution integrating a maia detector at beamline P06 at PETRA III. *J. Synchrotron Radiat.* **23**, 1550–1560 (2016).
41. W. De Nolf, F. Vanmeert, K. Janssens, XRDUA: Crystalline phase distribution maps by two-dimensional scanning and tomographic (micro) x-ray powder diffraction. *J. Appl. Cryst.* **47**, 1107–1117 (2014).
42. M. Ledésert, J. C. Monier, Crystal structures of $KCdCl_3{\cdot}H_2O$ and $KCdCl_3$. *Z. Kristallogr. Cryst. Mater.* **165**, 199–208 (1983).
43. M. D. Kumar, M. Rajendran, Salt effect on the enthalpy of mixing of water+methanol at 303.15 K. *Fluid Phase Equilib.* **164**, 217–224 (1999).
44. R. Christoph, B. Schmidt, U. Steinberner, W. Dilla, R. Karinen, *Ullmann's Encyclopedia of Industrial Chemistry* (Wiley-VCH, 2012), vol. 17, pp. 67–82.

Acknowledgments: We thank colleagues of the RCE for having provided the historical cadmium yellow pigment powder, Dr. Jan Garrevoet for assistance during beamtimes at DESY-P06, and all the staff of the Munch Museum (Conservation Department) for their collaboration. **Funding:** The research was financially supported by the European research project IPERION-CH, funded by the European Commission, H2020-INFRAIA-2014-2015 (grant agreement no. 654028); the project AMIS, within the program Dipartimenti di Eccellenza 2018-2022 (funded by MIUR and University of Perugia); and the program "Ricerca di Base 2017" (funded by University of Perugia). S.D.M. and K.J. acknowledge the GOA Project SolarPaint from the University of Antwerp Research Council and projects G056619N and G054719N from FWO (Brussels). F.V. and K.J. acknowledge support from Interreg Project Smart*Light and thank BELSPO (Brussels) for financial support via FED-tWIN mandate PRF055. L.M. acknowledges the Erasmus+ program (Staff Mobility for training, A. Y. 2018 to 2019) of the European Commission. In situ noninvasive analyses were performed using the European MOLAB platform, which is financially supported by the European project IPERION-CH. For the beamtime grants received, the authors thank the ESRF-ID21 beamline (experiment nos. HG32, HG64, and HG95), DESY-P06 beamline, a member of the Helmholtz Association HGF (experiment nos. I-20130221 EC and I-20160126 EC), and the project CALIPSOplus under the Grant Agreement 730872 from the EU Framework Programme for Research and Innovation HORIZON 2020. **Author contributions:** MOLAB investigations and data processing: L.M., L.C., F.R., C.G., I.C.A.S., R.P.d.F., A.R., and C.M. Experiments at SR facilities and data processing: L.M., A.C., S.D.M., G.N., F.V., M.C., K.J., W.D.N., G.F., and J.M. Data interpretation: L.M., L.C., F.R., K.J., A.R., I.C.A.S., E.S.T., and C.M. Manuscript writing: L.M., L.C., F.R., K.J., A.R., and C.M. All authors contributed to the revision of the manuscript. **Competing interests:** The authors declare that they have no competing interests. **Data and materials availability:** All data needed to evaluate the conclusions in the paper are present in the paper and/or the Supplementary Materials. Additional data related to this paper may be requested from the authors.

Submitted 13 June 2019
Accepted 6 March 2020
Published 15 May 2020
10.1126/sciadv.aay3514

Citation: L. Monico, L. Cartechini, F. Rosi, A. Chieli, C. Grazia, S. De Meyer, G. Nuyts, F. Vanmeert, K. Janssens, M. Cotte, W. De Nolf, G. Falkenberg, I. C. A. Sandu, E. S. Tveit, J. Mass, R. P. de Freitas, A. Romani, C. Miliani, Probing the chemistry of CdS paints in *The Scream* by in situ noninvasive spectroscopies and synchrotron radiation x-ray techniques. *Sci. Adv.* **6**, eaay3514 (2020).

Probing the chemistry of CdS paints in *The Scream* by in situ noninvasive spectroscopies and synchrotron radiation x-ray techniques

Letizia Monico, Laura Cartechini, Francesca Rosi, Annalisa Chieli, Chiara Grazia, Steven De Meyer, Gert Nuyts, Frederik Vanmeert, Koen Janssens, Marine Cotte, Wout De Nolf, Gerald Falkenberg, Irina Crina Anca Sandu, Eva Storevik Tveit, Jennifer Mass, Renato Pereira de Freitas, Aldo Romani and Costanza Miliani

Sci Adv **6** (20), eaay3514.
DOI: 10.1126/sciadv.aay3514